Molecular Mechanics Calculations and Molecular Dynamics Simulations of Biological Systems

李桂仁
Kuei-Jen Lee
德育醫護管理專科學校

Abstract

Molecular dynamics simulation of the 3′-cytidine monophosphate (3′-CMP)/RNase A complex has been carried out at three temperatures, 273K, 300K, and 323K. The trajectories obtained allowed us to calculate the dynamics of 3′-CMP in protein complex. The O−P bond was found to exert angular fluctuation of magnitudes 20^o, 26^o, and 30^o at 273K, 300K, and 323K, respectively. These values compare quite favorably with that obtained from lineshape simulation of the ^{31}P NMR powder patterns. A computer search with molecular mechanics calculations is applied to determine the possible low-energy configurations of two adjacent molecules, $CAP18_{106-137}$ and lipid A. This computer search is performed by systematically searching the five degrees of freedom that define the relative orientations of the two adjacent molecules. Hydrophilic and hydrophobic units are separated into several small domains along the $CAP18_{106-137}$ molecule so that it can interact with the lipid A either through the Coulombic interactions with the diphosphoryl head group or through the hydrophobic interactions with the fatty acyl chains. The intermolecular interactions are calculated through the van der Waals and Coulombic interactions. The Coulombic interactions are calculated by using a dielectric constant either with a value of unity $\epsilon = 1$ or with a distance-dependent dielectric function $\epsilon(r) = r_{ij}$. Based on the 400 lowest searched configurations, the intermolecular interactions calculated with $\epsilon = 1$ are found to be about sevenfold lower than those calculated with $\epsilon(r) = r_{ij}$.

I. Introduction

Macromolecules are dynamic systems which undergo fluctuations through several conformational substates.[1,2] These conformational fluctuations are important for biological functions, including enzyme catalysis and receptor binding. Experimentally such dynamical information has been inferred from analysis of the structural factors in X-ray crystal structures,[3] from lineshape simulations of solid state NMR powder patterns[4] due to anisotropic interactions, and from order parameters deduced from heteronuclear NMR relaxation measurements.[5] Theoretical molecular dynamics (MD) simulation has been demonstrated to be a powerful tool in studying the dynamical behavior of macromolecules.[6,7] In this study we report an MD simulation study of the dynamical behavior of a ligand, 3′-cytidine monophosphate (3′-CMP) (Fig. 1) bound to the protein ribonuclease A (RNase A) from pancreas. Several 500 ps MD simulations have been conducted to determine the dynamics of 3′-CMP in protein complex based on coordinates of the crystal structure of RNase A/Vanadate monophosphate deposited in Brookhaven protein data bank. We observed large amplitude angular fluctuation of the phosphate group consistent with that observed by lineshape simulation of the ^{31}P NMR powder pattern of polycrystalline 3′-CMP/RNase complex (Fig. 2).[8]

Lipopolysaccharides (LPSs) form the main constituents of the outer leaflet of the outer membrane of Gram-negative bacteria.[9] LPSs are known as a major factor of bacterial toxin due to Gram-negative infections and are termed endotoxins.[10] LPSs are composed of a polysaccharide part which is covalently attached to a lipid A (Fig. 3).[11] The polysaccharide part can be divided into two regions[12]: one is the *O*-specific chain that is variable by different Gram-negative bacterial species, and the other is the core oligosaccharide that is less variable. The lipid A is an amphiphilic molecule consisting of a charged diphosphoryl glucosamine head group and this hydrophilic group is linked up to seven hydrophobic fatty acyl chains via ester or amide linkages. Endotoxins of Gram-negative bacteria cause a serious complication of inflammation in humans. Therefore, a reasonable approach to

controlling the inflammation is to eliminate the harmful effects of LPSs by neutralizing the endotoxins.[13] CAP18 (cationic antimicrobial protein, 18kd)[14] is a novel protein which has been shown to bind to and inhibit various LPS activities. CAP18 was first isolated from rabbit granulocytes[15] and its amino acid sequence, as deduced from cDNA clones, shows a protein of 142 residues.[14] This protein consists of two domains: one is an N-terminal domain of unknown function, and the other is a C-terminal domain of 37 amino acids ($CAP18_{106-142}$) having LPSs binding activity.[16] This peptide has a broad antimicrobial activity versus both Gram-positive and Gram-negative bacteria. Recently, a peptide fragment, corresponding to residues 106-125 ($CAP18_{106-125}$)[17] was identified and shown to display a potent bacterial activity against both Gram-negative and Gram-positive bacteria. A more potent fragment of peptide, $CAP18_{106-137}$, was isolated and identified by Larrick et al.[18] and used for this work. The structure of the $CAP18_{106-137}$ (Fig. 4) has been investigated by Huang and coworkers,[19] employing circular dichroism (CD) and solution nuclear magnetic resonance (NMR) techniques. With a certain amount of lipid A in the $CAP18_{106-137}$ aqueous solution, a helix structure was observed by CD spectra. This helix structure is similar to that determined in the presence in 30% (v/v) trifluoroethanol (TEF) by two-dimensional NMR.[19] A computer search with molecular mechanics calculations,[20] which has been used to study cholesterol-cholesterol intermolecular interactions, is chosen as the tool to identify the possibly low interaction energies of relative orientations for the $CAP18_{106-137}$ and lipid A molecules.

II. Results and Discussion

(1) Angular fluctuation of the O–P bond:

The spatial orientation of the phosphate group is defined by the angle θ, which is calculated from the following equation:

$$\mathbf{A} \cdot \mathbf{B} = |A||B| cos\ \theta, \tag{1}$$

where **A** is the initial O−P bond vector which is defined by the coordinates of the O and P atoms at $t = 0$. Vector **B** is the instantaneous vector which is defined by the instantaneous coordinates of the O and P atoms at subsequent time t, calculated from the MD simulations. Thus at initial time, $t = 0$, θ equals to 0. θs determined from the 500 ps MD simulation at 323K are shown in 0.2 ps time steps in Fig. 5. The statistics, i.e. the frequency of the O−P bond orienting at certain angle θ, in 2 degree resolution at 323 K was shown in Fig. 6. Also shown in Fig. 6 are the corresponding angular distribution curves of the O−P bond obtained from MD simulations at 273 and 300 K.

The three distribution curves have the appearance close to that of Gaussian distributions. The amplitudes of the fluctuations of these three distribution curves can be specified by the full width at half height, $\Delta\theta_{1/2}$ of the curves and are found to be 10°, 13°, and 15° at 273K, 300K, and 323K, respectively. Since the angles calculated from equation (1) are solid angles the maximal angular fluctuation can be twice of $\Delta\theta_{1/2}$, or 20°, 26°, and 30° at 273K, 300K, and 323K, respectively. These values agree quite well with the estimated 30° fluctuation of the O−P bond obtained from lineshape simulation of the ^{31}P NMR spectra of 3′-CMP/RNase A complex in polycrystalline state.[8]

(2) Angular fluctuation of the dihedral angle defined by P−$O_{3'}$−$C_{3'}$−$C_{4'}$:

The rotational isomeric states are characterized by dihedral angles. We have monitored the angular fluctuation of the dihedral angle specified by the P−$O_{3'}$−$C_{3'}$−$C_{4'}$ bonds. Fig. 7 is shown the histogram of the dihedral angle fluctuation about the ϵ bond at 323K. Fig.8 shows the populational distribution of the dihedral angle calculated from MD simulation at 273K, 300K, and 323K. The cueves all show a single Gaussian-like distribution. The full width at half height of the distribution are about 20°, 22°, and 25° at 273K, 300K, and 323K, respectively. Thus, unlike the rapid *trans-gauche* isomerization observed in polymethylene chain[21] due to low energy barrier, large angle dihedral angle fluctuation

($\geq 60°$) about the ϵ bond occurs very rarely in the present case. However, it should be pointed out that the present study do not provide any clue of the populational distribution of *trans* or *gauche* state. It merely shows that transition between these two states does not occur often within the 500 ps time period.

Similar MD calculations were also carried out at 273K, 300K, and 323K for the same segment of 3′-CMP in protein-free state. Such simulation allows us to assess the effect of protein on motional freedom of the ligand. The angular distribution for all three temperatures are shown in Fig. 9. In comparison, two aspects distinguish the dynamical behavior between the protein-free and protein-bound states: (i) The maxima of the distribution curves in the protein-free state occur at 110° instead of 190° observed in the protein-bound state. Thus the ligand conformation in the bound state is highly dependent of the protein environment. (ii) Unlike the single Gaussian-like distribution occurred in the protein-bound state a second maximum of about half the probability at 150° was observed in all three distribution curves in the protein-free state. From the populational distributions of the two states one can estimate the energy differences between these two states from the Arrhenius equation $\Delta G = -RTlnK$. The best estimate is about 0.4 Kcal/mol, which is quite close to that expected for polymethylene chain. These results testify the ultimate importance of the protein environment in restricting the motional freedom of the ligand.

(3) Molecular Associations:

The $CAP18_{106-137}$ and lipid A were treated as rigid molecules in the search procedure. The intermolecular interactions were calculated only the atomic pairs from the two different molecules, and the pairwise interactions were calculated according to Eqs. (2) and (3).

$$E_{ij} = \varepsilon_{ij}\left[2\left(\frac{r^*_{ij}}{r_{ij}}\right)^9 - 3\left(\frac{r^*_{ij}}{r_{ij}}\right)^6\right], \qquad (2)$$

where ε_{ij} is the well depth in kcal/mol, r^*_{ij} is the interatomic distance in Å at which the

minimum energy can be obtained, and r_{ij} indicates the distance between atoms i and j.

$$E_{coul} = C_0 q_i q_j / (\epsilon r_{ij}), \tag{3}$$

where q_i and q_j are the charges in electron units, r_{ij} is the distance in Å, ϵ is the dielectric constant, and E_{coul} is in kcal/mol when $C_0 = 332.06$. Of the searched results, only the lowest 400 of the total number of configurations were printed out. Figs. 10 and 11 depict the calculated energies as a function of the 400 configurations for the dielectric constants $\epsilon = 1$ and $\epsilon(r) = r_{ij}$, respectively. These figures show that these energies, when $\epsilon = 1$, are about sevenfold lower than those calculated with $\epsilon(r) = r_{ij}$ so that the Coulombic interactions are the dominant factors causing the molecular associations in these 400 configurations. The $CAP18_{106-137}$ molecule possesses 13 positive charges, which come from lysine and arginine residues at pH 3.5,[19] and these residues are located near the N-terminus. On the other hand, the lipid A molecule carries two negative charges at the two phosphoryl groups. Thus, there are several possible positions for the favorable interactions between the charged residues and the phosphoryl groups, and the Coulombic interactions are more important than the van der Waals. In addition, interactions are possibly exhibited between hydrophobic residues located near the C-terminus and the fatty acyl chains of the lipid A via the van der Waals (hydrophobic) interactions. To understand the molecular associations, for example, the configuration with the lowest interaction energy (−700.5 cal/mol) was observed thoroughly. Fig. 12 depicts this configuration in which four charged residues (lysines) of the peptide interact with the phosphoryl groups of the lipid A via Coulombic interactions.

III. Conclusions

Small amplitude fluctuation of < 1Å plays significant role in biological processes such as enzyme catalysis. A change of 0.1 or 0.3Å was proposed to cause an change in reaction rate by a factor of 3 or 5,000, respectively.[22,23] This corresponds to an increase in activation

energy of 0.7 and 5.0 Kcal/mol. Thus, the information gleaned from either experiment or theory argues for the importance of small molecular changes on the order < 1Å. The present MD calculations are limited to atoms within a 15Å radius of the phosphate atom. Larger amplitude fluctuation is expected when the calculation is extended to the whole molecule. Even with this limited MD calculation we can gain detailed insight into the dynamical behavior of a ligand bound to the active site of the protein. The ligand was found to be rather dynamic. Large amplitude fluctuations of the O−P bond are predicted from our simulation, and confirmed by NMR. The three distribution functions of the dihedral angles specified by $P-O_{3'}-C_{3'}-C_{4'}$ assume a Gaussian shape with the maxima occur at an angle corresponding to a *trans* configuration.

The binding of the $CAP18_{106-137}$ to the lipid A, studied experimentally by Huang and coworkers,[19] has been studied with the aid of molecular mechanics modeling. Molecular mechanics modeling by means of a computer search has made it possible to calculate the intermolecular interactions of $CAP18_{106-137}$/lipid A associations and find the possibly favorable arrangements between these two adjacent molecules. The calculated results indicate that the Coulombic interactions are favorable either when the value of the dielectric constant is unity or when the dielectric constant is distance-dependent, i.e., the highly cationic domain near the N-terminus of the peptide reacting with the diphosphoryl groups of the lipid A is significant. This finding suggests that interactions carried out in this region may play an essential role in biological functions. However, the number of hydrophobic interactions increases if the distance-dependent dielectric function is used, i.e., the fatty acyl chains of lipid A have a tendency toward the hydrophobic domain near the C-terminus of the peptide.

References

1. Gurd, F. R. N.; Rothgeb, T. M. *Adv. Protein Chem.* **1979**, *33*, 74.
2. Karplus, M.; McCammon, J. A. *Sci. Am.* **1986**, *254(4)*, 42.
3. Chang, S.-L. *Multiple Diffraction of X-Rays in Crystal*; Springer-Verlag: New York, 1984.
4. Griffin, R. G.; Beshah, K.; Ebelhauser, R.; Huang, T.-h.; Olejnizak, E. T.; Rice, D. M.; Siminovitch, D. J.; Wittebort, R. J. In *The Time Domain in Surface and Structural Dynamics*; Long, J.; Grandjean, F., Eds.; Kluwer Academic Pub.: New York, 1988; p 81-105.
5. Lipari, G.; Szabo, A. *J. Am. Chem. Soc.* **1982**, *104*, 4559.
6. McCammon, J. A.; Harvey, S. C. *Dynamics of Proteins and Nucleic Acids*; Cambridge University Press: New York, 1987.
7. Brooks III, C. L.; Karplus. M.; Pettitt, B. M. *Adv. Chem. Phys.* **1988**, *71*, 1.
8. Huang, T.-h.; Griffin, R. G.; Petsko, G. A., (unpublished results).
9. Raetz, C. R. H. *Annu. Rev. Biochem.* **1990**, *59*, 129.
10. Westphal, O.; Westphal, U.; Sommer, Th. In *Microbiology-1977*; Schlessinger, D., Ed; American Society for Microbiology: Washington, D.C., 1978; pp. 221-238.
11. Luderitz, O.; Freudenberg, M. A.; Galanos, C.; Lehmann, V.; Rietschel, E. Th.; Shaw, D. H. *Curr. Top. Membr. Transp.* **1982**, *17*, 79.
12. Hitchcock, P. J.; Leive, L.; Makela, H.; Rietschel, E. Th.; Strittmacher, W.; Morrison, D. C. *J. Bacteriol.* **1986**, *166*, 699.
13. Morrison, D. C.; Ryan, J. L. *Annu. Rev. Med.* **1987**, *38*, 417.
14. Larrick, J. W.; Morgan, J. G.; Palings, I.; Hirata, M.; Yen, M. H. *Biochem. Biophys. Res. Commun.* **1991**, *179*, 170.
15. Hirata, M.; Yoshida, M.; Inada, K.; Kirkae, T. *3rd International Endotoxin Conference* **1988**, Amsterdam, The Netherlands.
16. Larrick, J. W.; Hirata, M.; Zheng, H.; Zhong, J.; Bolin, D.; Cavaillon, J,-M.; Warren,

H. S.; Wright, S.C. *J. Immunol.* **1994**, *152*, 231.

17. Tossi, A.; Scocchi, M.; Skerlavaj, B.; Gennaro, R. *FEBS Lett.* **1994**, *339*, 108.
18. Larrick, J. W.; Hirata, M.; Shimomoura, Y.; Yoshida. M.; Zheng, H.; Zhong, J.; Wright, S.C. *Antimicrob. Agents Chemother.* **1993**, *37*, 2534.
19. Chen, C.; Brock, R.; Luh, F.; Chou, P.-J.; Larrick, J. W.; Huang, R.-F. Huang, T.-h. *FEBS Lett.* **1995**, *370*, 46.
20. Liang, C.; Yan, L.; Hill, J.-R.; Ewig, C. S.; Stouch, T. R.; Hagler, A. T. *J. Comput. Chem.* **1995**, *16*, 883.
21. Flory, P. J. *Statistical Mechanics of Chain Molecules*; Interscince: New York, 1969.
22. Wu, Y. D.; Houk, K. N. *J. Am. Chem. Soc.* **1987**, *109*, 2226.
23. Benkovic, S. J.; Fierke, C. A.; Naylor, A. M. *Science* **1988**, *239*, 1105.

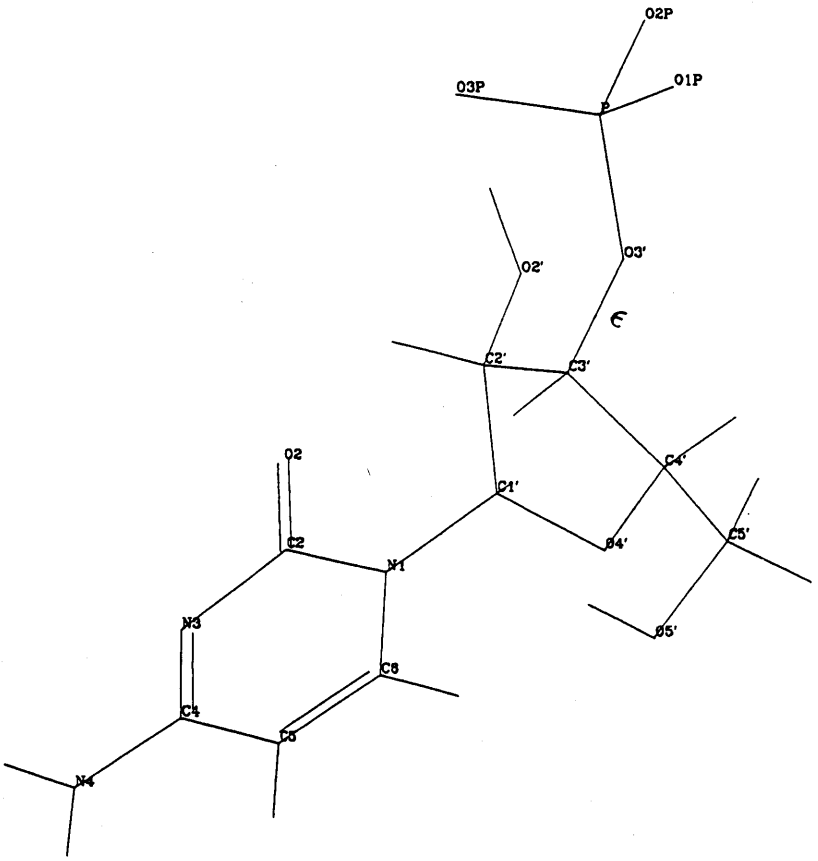

Fig. 1 The chemical structure of 3′-cytidine monophosphate. There are no labels on hydrogen atoms.

Fig. 2 Ligand (heavy lines) and part of ribonuclease A structure for the simulation system, located within 15 Å of the phosphate atom.

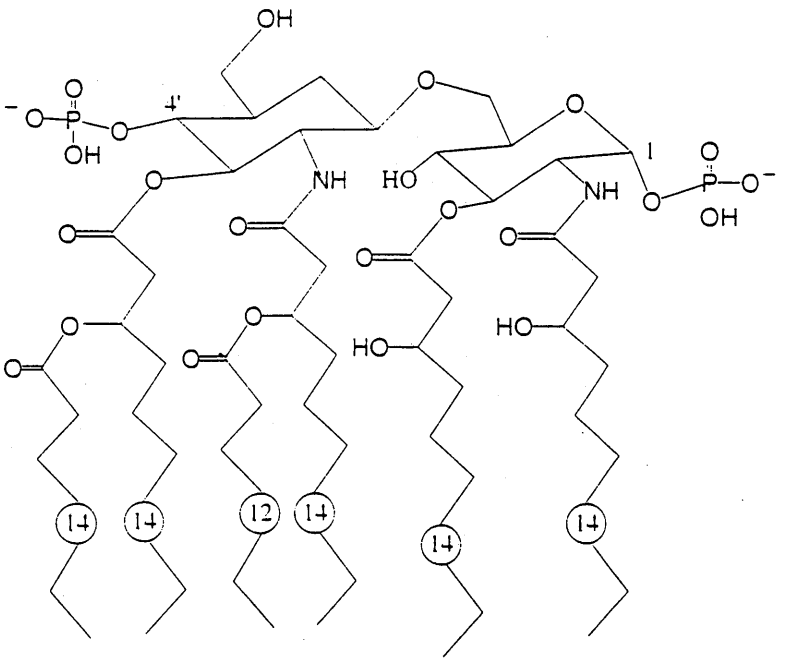

Fig. 3 Chemical structure of the lipid A. Numbers in circles denote the length of fatty acyl chains.

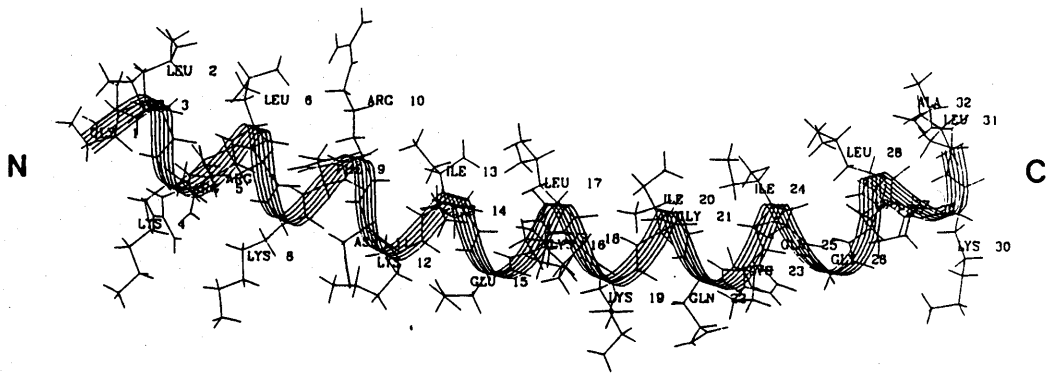

Fig. 4 A helical structure of the $CAP18_{106-137}$.

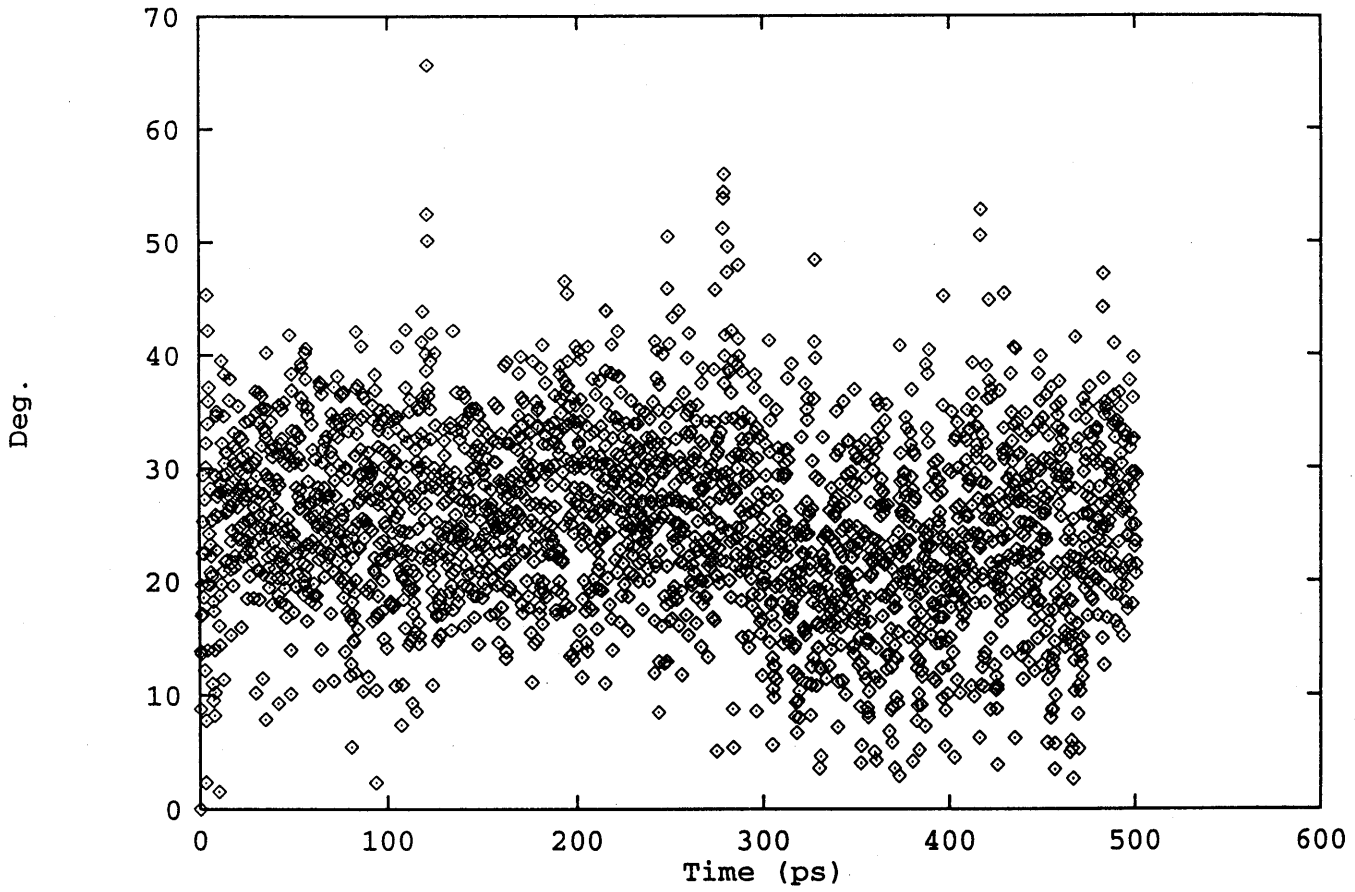

Fig. 5 Instantaneous angles of the O−P bond determined with respect to the initial orientation of the O−P bond of 3′-cytidine monophosphate. Simulation was performed at 323 K.

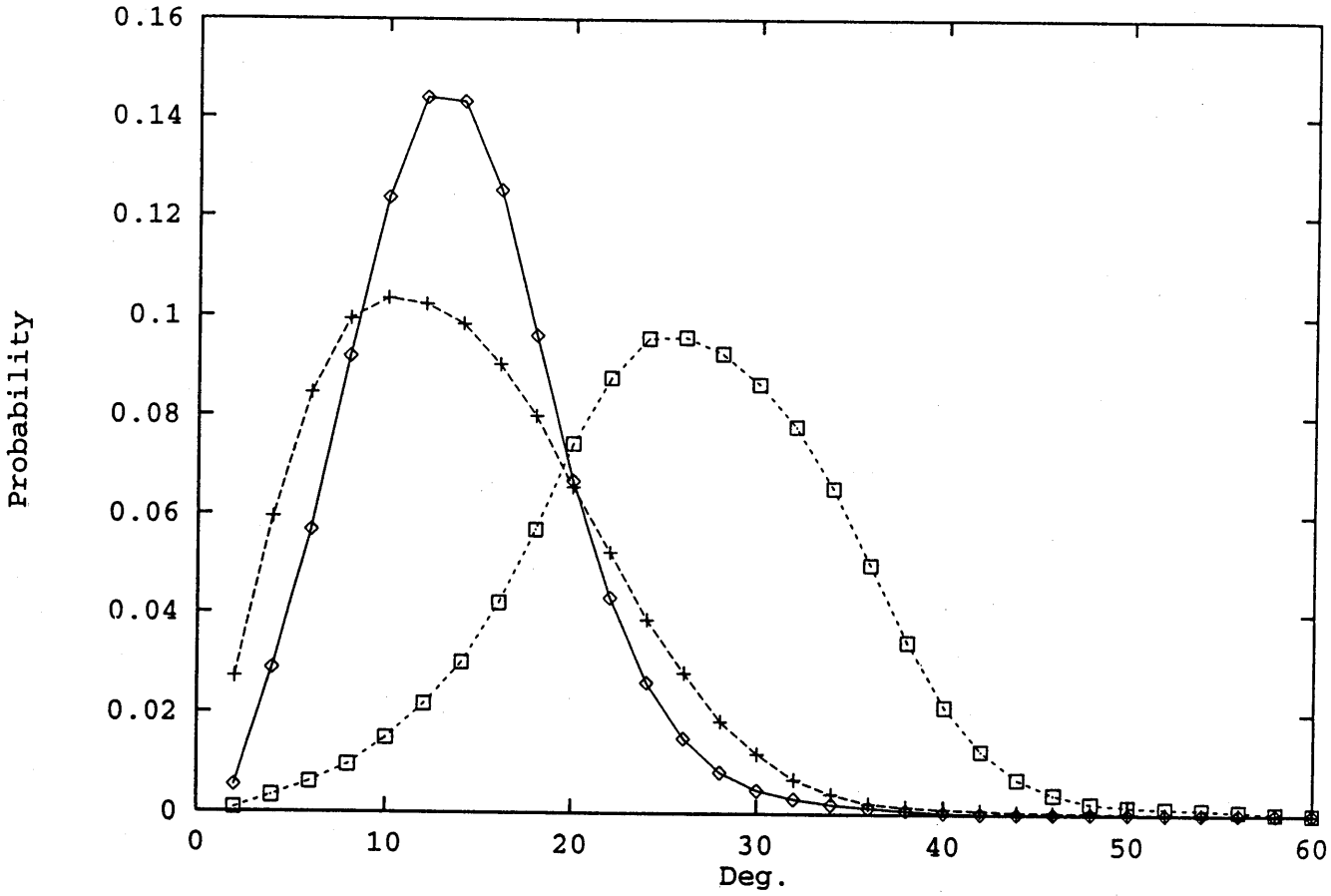

Fig. 6 Angular distribution functions of the O−P bond simulated at three different temperatures: 273 K (◇), 300 K (+), and 323 K (□).

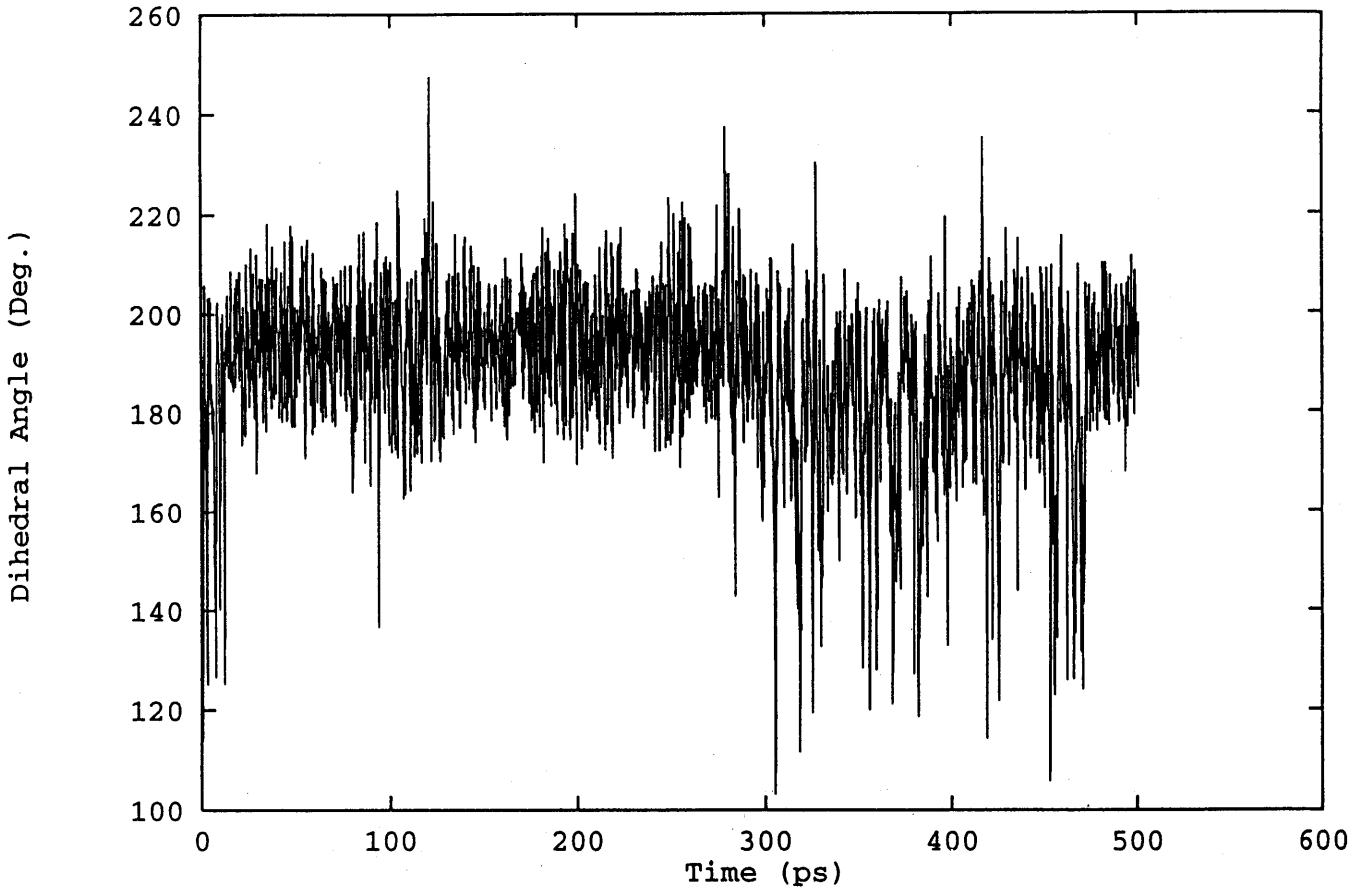

Fig. 7 (a)Histogram of the dihedral angle at the ϵ bond of 3′-cytidine monophosphate. Simulation was performed at 323 K.

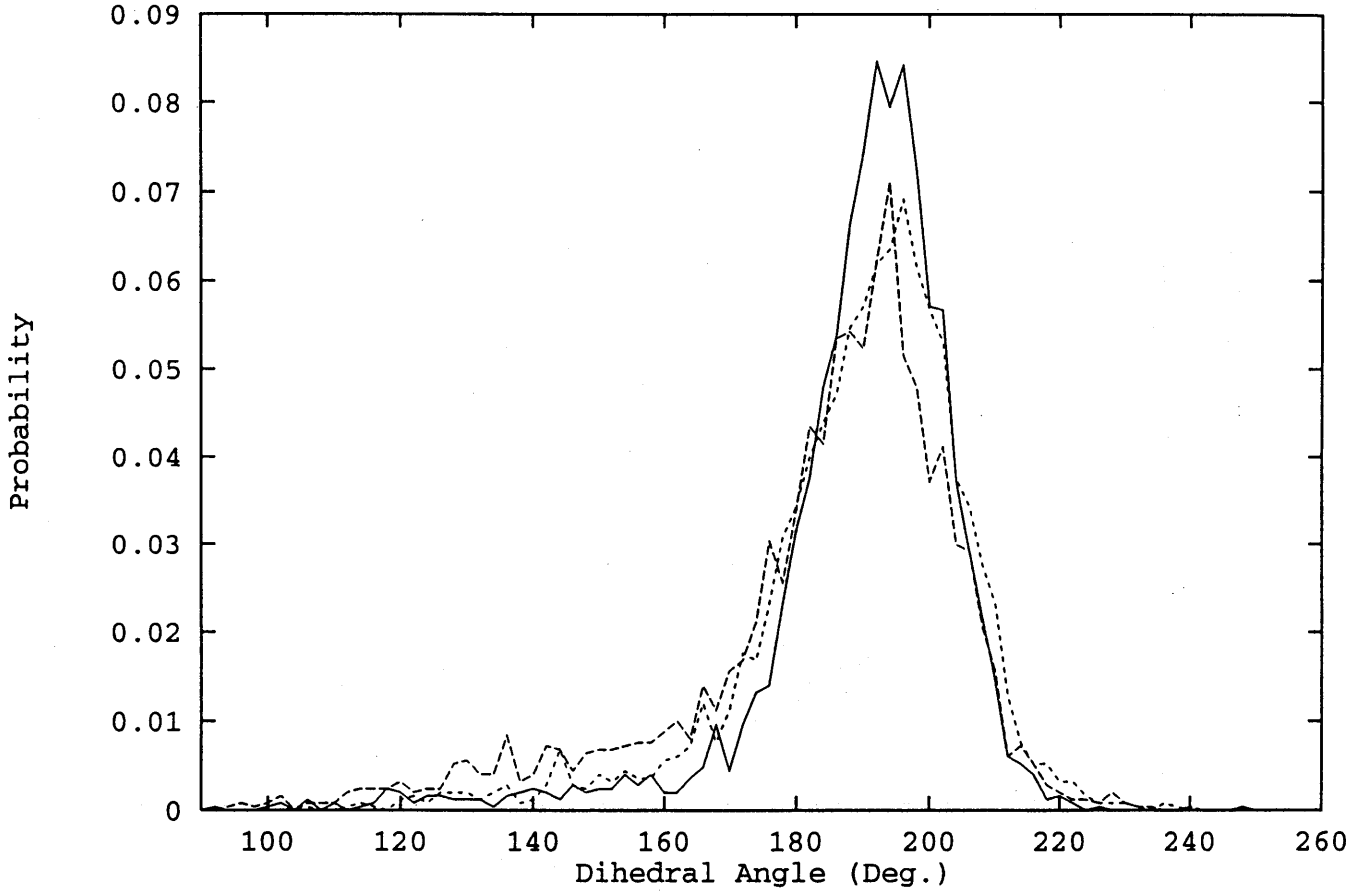

Fig. 8 Distribution functions for the dihedral angle at the ϵ bond of 3′-cytidine monophosphate. Simulationis were performed at three different temperatures: 273 K (solid curve), 300 K (dashed curve), and 323 K (dotted curve).

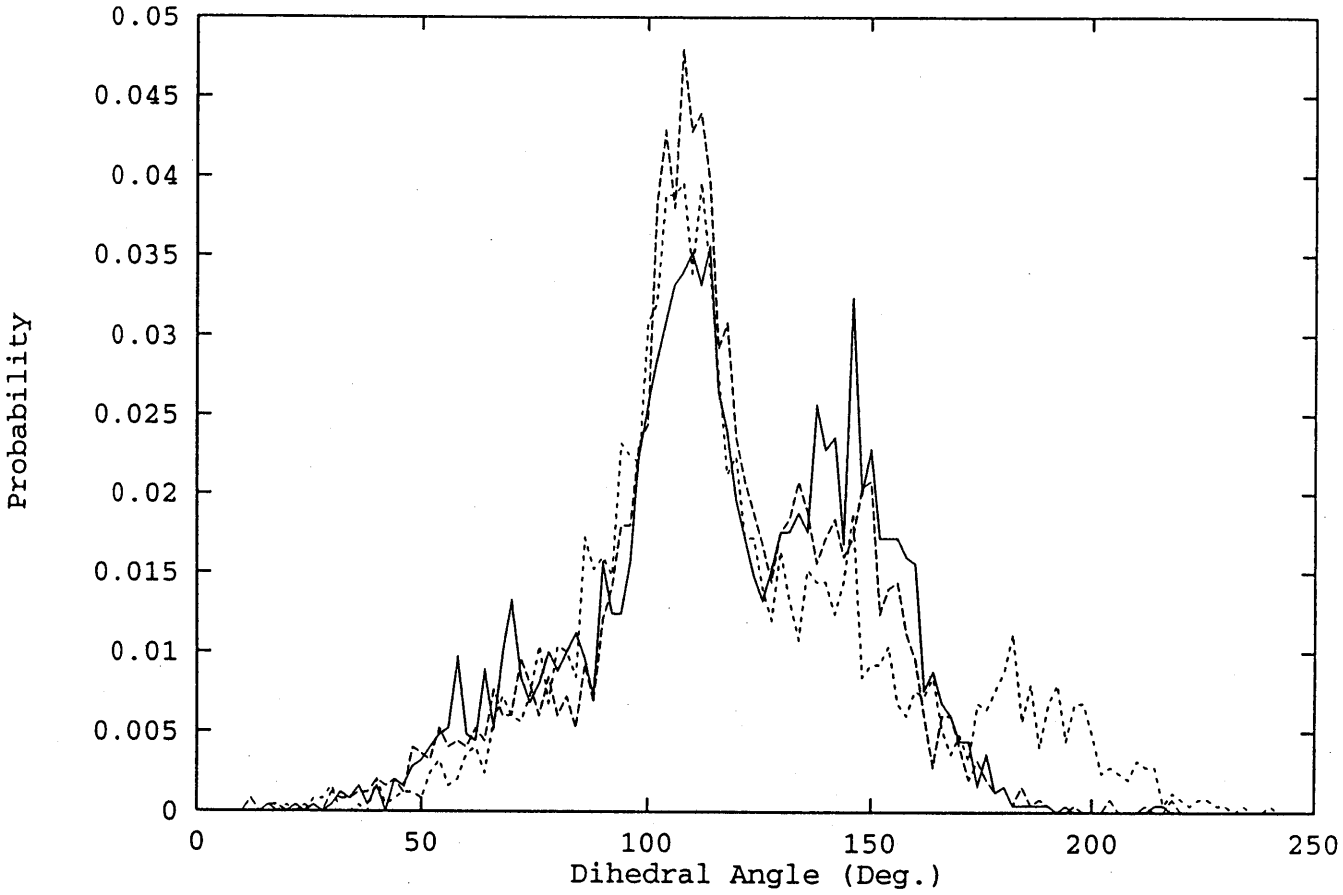

Fig. 9 Distribution functions for the dihedral angle at the ϵ bond of 3′-cytidine monophosphate. Simulationis were performed in vacuo and at three different temperatures: 273 K (solid curve), 300 K (dashed curve), and 323 K (dotted curve).

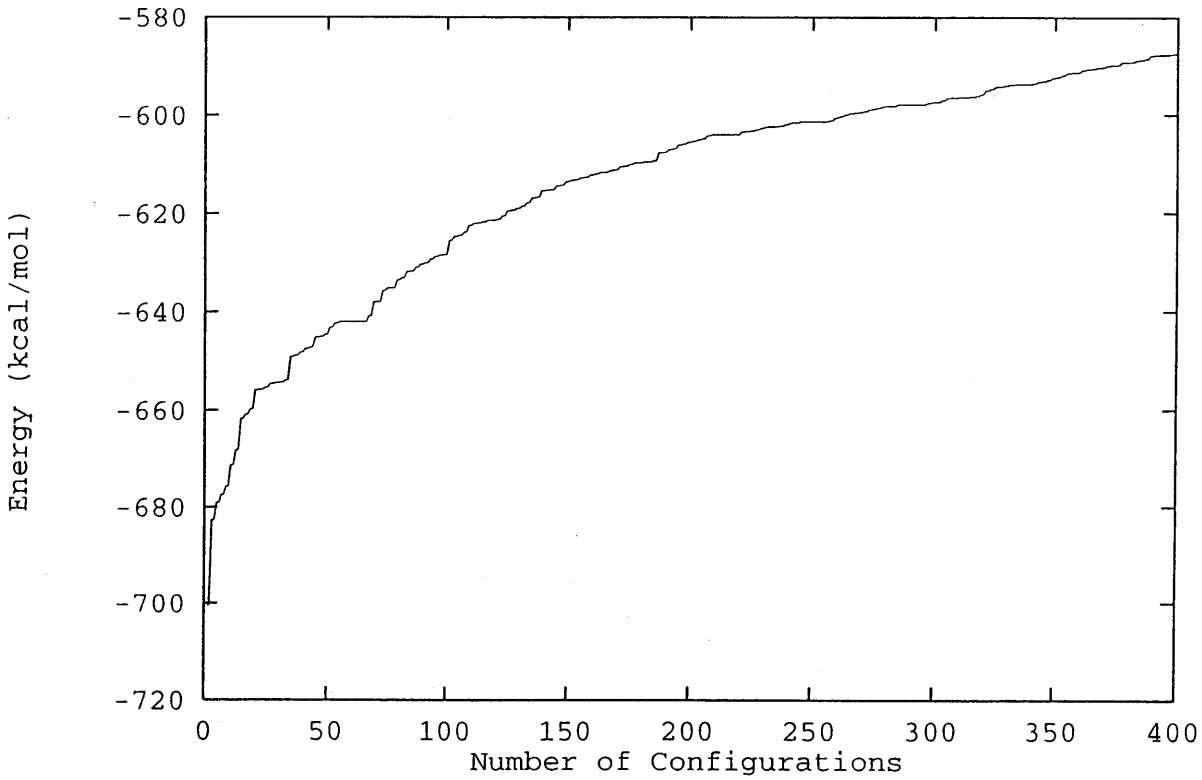

Fig. 10 Plot of interaction energy *vs.* the number of configurations. The Coulombic interactions were calculated with $\epsilon = 1$.

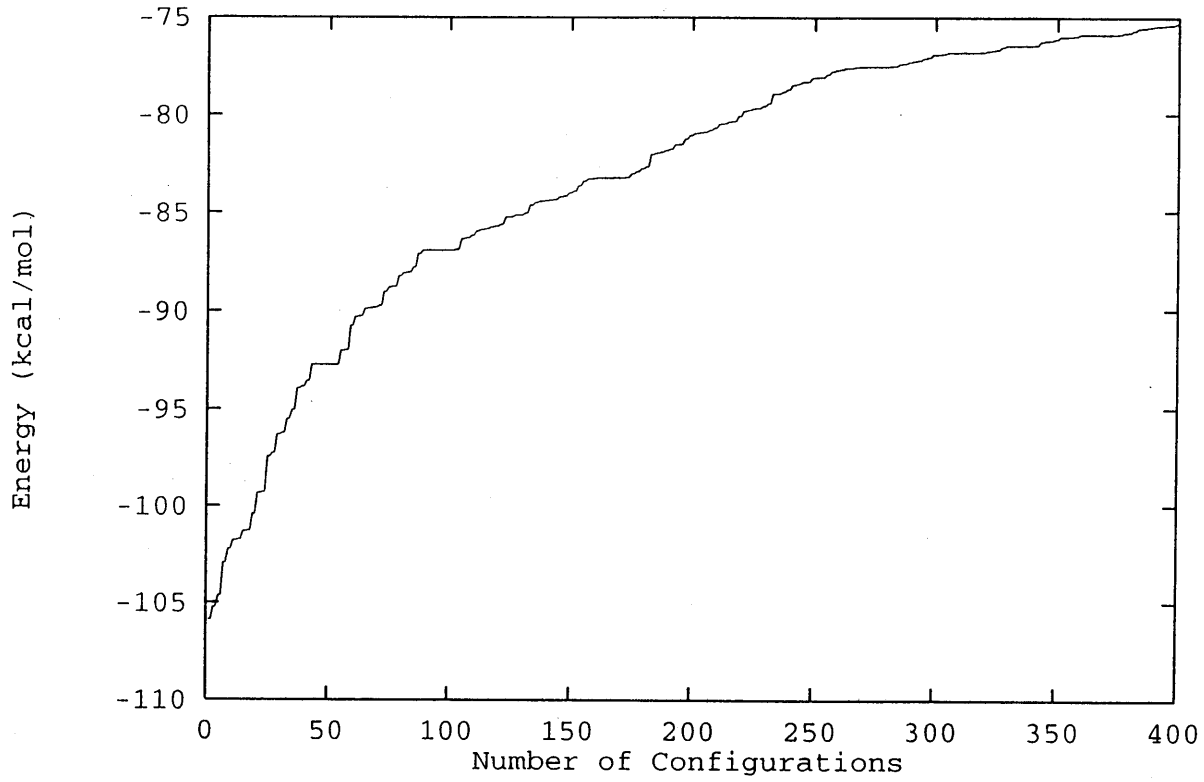

Fig. 11 Plot of interaction energy *vs.* the number of configurations. The Coulombic interactions were calculated with $\epsilon(r) = r_{ij}$.

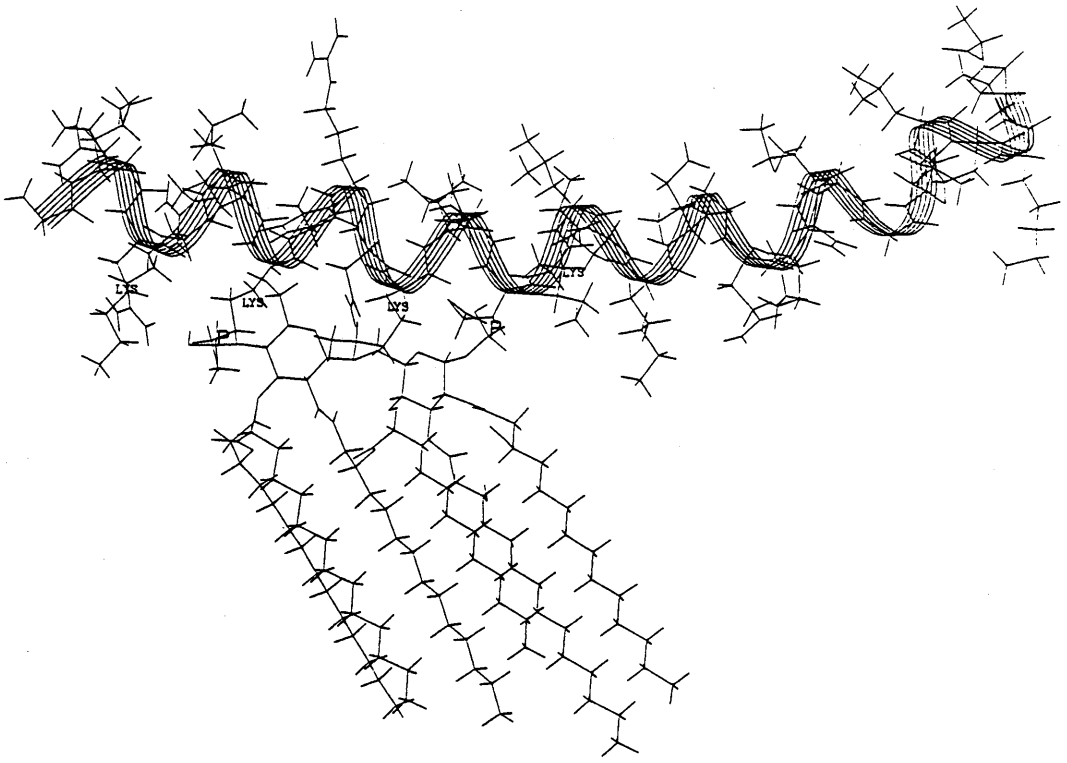

Fig. 12 The snapshot for the lowest intermolecular interaction (−700.5 cal/mol) of the 400 searched configurations for the $CAP18_{106-137}$/lipid A complex. The Coulombic interactions were calculated with $\epsilon = 1$.